RESEARCH ARTICLE | NOVEMBER 13 2023

Growth of tin-free germanium carbon alloys using carbon tetrabromide (CBr $_{\!\scriptscriptstyle 4}$) $\ensuremath{ \odot}$

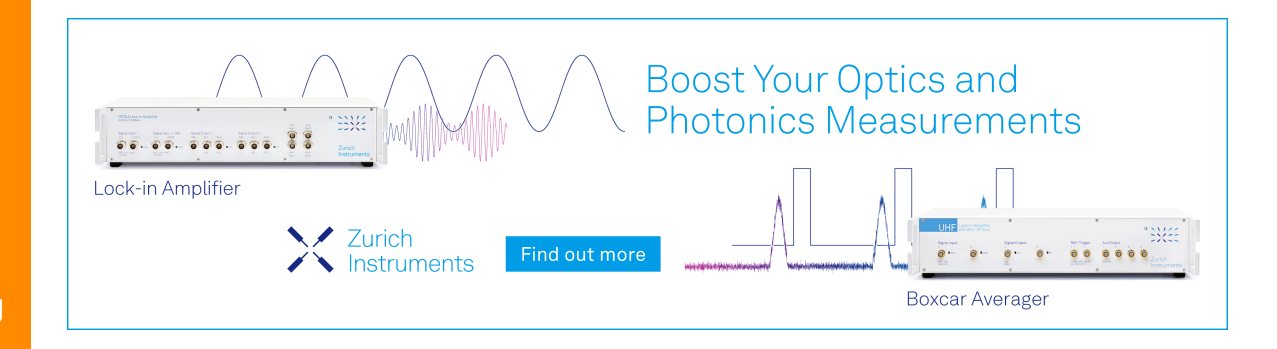
Md. Shamim Reza ⑩ ; Tuhin Dey ⑩ ; Augustus W. Arbogast ⑩ ; Aaron J. Muhowski ⑩ ; Mark W. Holtz ⑩ ; Chad A. Stephenson ⑩ ; Seth R. Bank ⑩ ; Daniel Wasserman ⑩ ; Mark A. Wistey ➡ ⑩



J. Appl. Phys. 134, 183103 (2023) https://doi.org/10.1063/5.0172330









Growth of tin-free germanium carbon alloys using carbon tetrabromide (CBr₄)

Cite as: J. Appl. Phys. 134, 183103 (2023); doi: 10.1063/5.0172330

Submitted: 14 August 2023 · Accepted: 21 October 2023 ·

Published Online: 13 November 2023







Md. Shamim Reza, 1 D Tuhin Dey, 1 D Augustus W. Arbogast, 2 D Aaron J. Muhowski, 3.4 D Mark W. Holtz, 1.2 D Chad A. Stephenson, ⁴ Seth R. Bank, ³ Daniel Wasserman, ³ and Mark A. Wistey 1,2,a)

AFFILIATIONS

- ¹Materials Science, Engineering, and Commercialization Program, Texas State University, San Marcos, Texas 78666, USA
- ²Department of Physics, Texas State University, San Marcos, Texas 78666, USA
- ³Department of Electrical and Computer Engineering, University of Texas at Austin, Austin, Texas 78712, USA

ABSTRACT

Direct bandgap group IV materials could provide intimate integration of lasers, amplifiers, and compact modulators within complementary metal-oxide-semiconductor for smaller, active silicon photonics. Dilute germanium carbides (GeC) with \sim 1 at. % C offer a direct bandgap and strong optical emission, but energetic carbon sources such as plasmas and e-beam evaporation produce defective materials. In this work, we used CBr₄ as a low-damage source of carbon in molecular beam epitaxy of tin-free GeC, with smooth surfaces and narrow x-ray diffraction peaks. Raman spectroscopy showed substitutional incorporation of C and no detectable sp² bonding from amorphous or graphitic carbon, even without surfactants. Photoluminescence shows strong emission compared with Ge.

Published under an exclusive license by AIP Publishing. https://doi.org/10.1063/5.0172330

I. INTRODUCTION

Direct bandgap group IV materials are highly desirable for active silicon photonic devices such as lasers and amplifiers because of the prospective ease of integration with Si, strong optical emission, and amplification, all intimately integrated very close to CMOS devices, without a separate wafer or die bonding. Band structure engineering of Ge alloys can overcome the small 0.14 eV difference between the conduction band direct (Γ) valley and indirect (L) valley.

The two most common routes to create a direct bandgap in group IV alloys are tensile strain in Ge¹⁻⁴ and alloying Ge with other group IV materials. 5-10 Several research groups have shown direct bandgap and optical emission from tensile strained Ge both theoretically and experimentally. Unfortunately, demonstrated lasers required high current density, and tensile Ge showed a tendency to degrade by forming dark line defects, i.e., dislocations. 16

Successful epitaxial growth of GeSn has also been demonstrated.5-7,17,18 Reported electrically pumped lasers only operate cryogenically, pulsed, and with high current densities. 19-The bandgap of GeSn is only weakly direct, and a very light conduction band (CB) effective mass in the direct (Γ) valley $(m_{c\Gamma}^* \leq 0.025m_0)$ means that most electrons remain in the L valley, reducing differential gain and increasing free carrier absorption. Also, the light $m_{c\Gamma}^*$ reduces the directness when confined in a quantum well (QW). To avoid this, all lasers reported to date have used QWs at least 15 nm wide, but such wide wells allow multiple energy states within the QW, diluting the electrons across multiple states, which reduces gain.

In this work, we instead alloyed Ge with dilute amounts of C. The substitutional incorporation of C onto Ge lattice sites offers additional freedom to engineer the band structure, strain, and optical confinement. Computational modeling has shown a direct bandgap for dilute germanium carbide alloys for less than 1% of substitutional C in Ge. 9,10,22 The carbon state in $Ge_{1-x}C_x$ splits the CB edge into two different bands, E⁺ and E⁻. Ab initio calculations show that the direct E^- valley at Γ drops below the L valley by as much as 200 meV, creating a strongly direct bandgap.

Previous groups reported MBE growth of $Ge_{1-x}C_x$ at various growth temperatures ranging from 200–650 °C^{23–28} and carbon fractions from 0% to 10%. These showed poor C incorporation onto crystal lattice sites, and growth was often dominated by

⁴Now at Sandia National Laboratory, Sandia, New Mexico 87185, USA

a) Author to whom correspondence should be addressed: mwistey@txstate.edu

C-C defects and other carbon clusters, attributed to low solid solubility. Most reported experimental studies focused on the direct growth of Ge_{1-x}C_x on Si(001), and the substrate-induced strain led to relaxation beyond a few monolayers of growth. 24,25,28 Relaxed Ge_{1-x}C_x/Si(100) thick layers typically exhibit highly defective microstructures containing a large concentration of misfit dislocations, which act as a sink for incorporated carbon. Osten et al. used Sb as a surfactant to prevent Stranski-Krastanov island formation during the Ge_{1-x}C_x film on Si (001).^{24,29} Though a few groups have grown Ge_{1-x}C_x on Ge (001) substrates to produce a thick pseudomorphic layer and to avoid misfit dislocations, ^{23,30,31} ous attempts generally relied on sources of carbon that either emitted carbon clusters, such as laser or thermal vaporization, 32-5 or used high energy sources, such as plasmas or electron beams. ^{23–25,28,30} Despite frequent use in semiconductor processing, plasmas have long been known to cause deep level traps, 36 and they are particularly destructive to highly mismatched alloys (HMAs) such as $Ge_{1-x}C_x$ and $GaAs_{1-x}N_x$. For example, even in $GaAs_{1-x}N_x$, with its stronger bonds, we found defects from low-energy plasma ions reduced photoluminescence by 80%. 37,38 As a result, most films demonstrated to date showed very high defect densities, or even graphitic or amorphous carbon. There are few reports of optical emission from Ge_{1-x}C_x, although Dashiell et al. reported near-band-edge photoluminescence (PL) at 735 meV assisted by transverse acoustic (TA) phonons.3

GeC growth using tetrakis(germyl)methane was reported by several groups, but this precursor requires significant effort to synthesize. 39,40 In this work, we report the first use of commercially available, 99.99% pure CBr4 (Strem Chemicals) as a carbon precursor for pseudomorphic, tin-free $\mathrm{Ge_{1-x}C_x}$ growth by molecular beam epitaxy (MBE). The cracking of CBr4 is a low-energy process that allows breaking the C–Br bond on the substrate surface at low growth temperatures without damaging the surface. After cracking, $\mathrm{Br_2}$ evaporates from the surface, leaving individual carbon atoms rather than carbon chains or nanoclusters. All samples reported here were grown on semi-insulating GaAs to allow through-wafer optical probing. As shown below, x-ray diffraction (XRD), Raman spectroscopy, and photoluminescence (PL) all suggest good structural quality.

II. EXPERIMENTAL METHODS

The $Ge_{1-x}C_x$ films were grown in a Varian/Intevac Mod Gen II hybrid source MBE system. Epi-ready, non-intentionally doped GaAs was deoxidized *in situ* using thermally cracked H at 406 °C for 20 min. A sharp (2 × 4) diffraction pattern in reflection highenergy electron diffraction (RHEED, not shown) indicated an oxide-free, clean surface. Germanium (Ge) was deposited from a previously calibrated Knudsen source at ~3 nm/min, and carbon (C) was deposited using gas source CBr₄. Growth temperatures

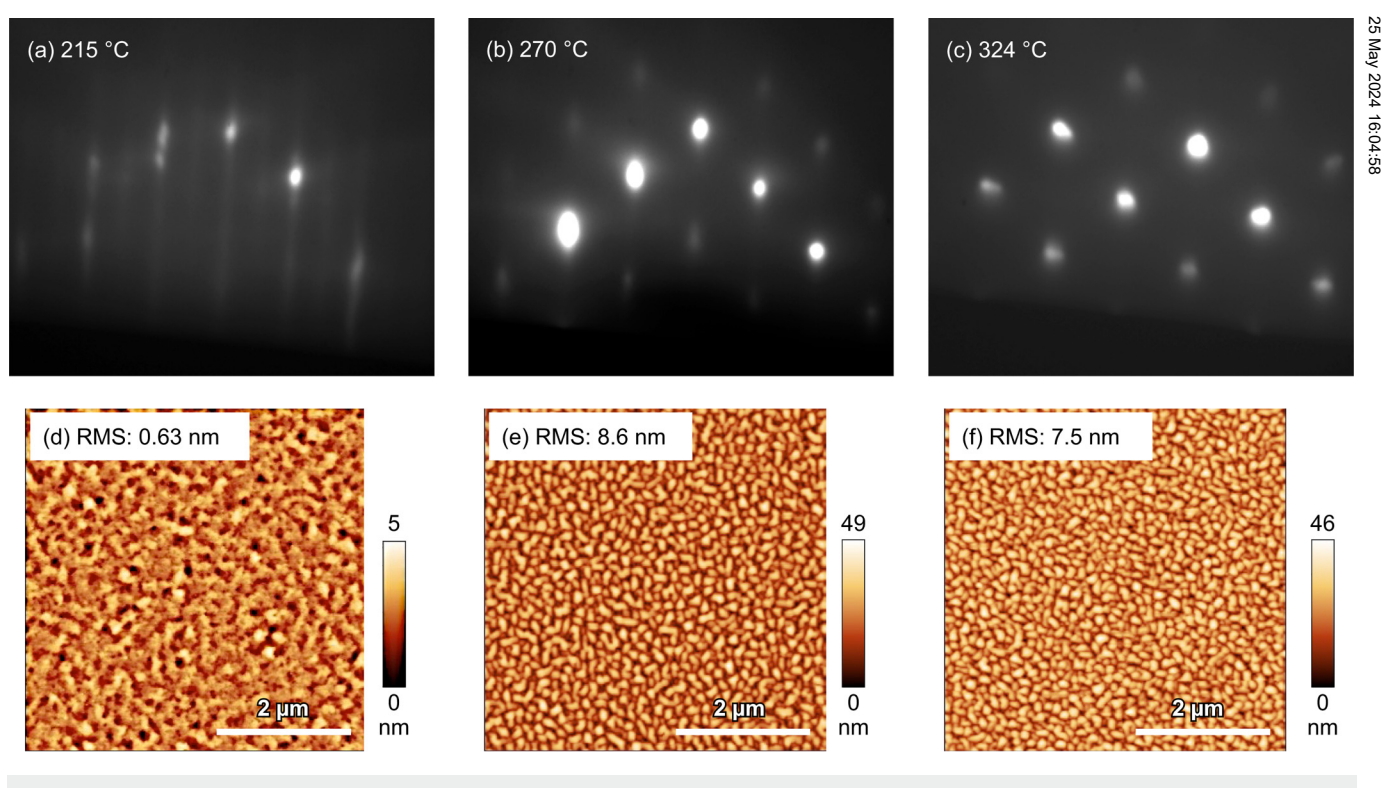


FIG. 1. (a)-(c) RHEED during Ge_{1-x}C_x active layer growth at 215, 270, and 324 °C, respectively. (d)-(f) Corresponding AFM.

reported here were calibrated by the melting point of indium droplets on Ge wafers.

Before growing the active layer of Ge_{1-x}C_x, we grew a 90 nm undoped Ge buffer layer at 406 °C, with sharp (2 × 2) reconstruction visible in RHEED. Following the buffer layer, we grew 170 nm of $Ge_{1-x}C_x$ at various temperatures for the active layer. The beam equivalent pressure of CBr_4 was 4.0×10^{-7} Torr, higher than that of Ge $(3.0 \times 10^{-7} \text{ Torr})$ due to the lower sticking coefficient of CBr₄. Finally, growths were concluded with a 10 nm Ge cap layer grown at 401 °C to aid with carrier confinement.

III. RESULTS AND DISCUSSION

RHEED was used to monitor real-time surface reconstruction during growth. The growth temperature of the Ge buffer was consistent for all samples, and we observed a sharp, (2×2) streaky RHEED pattern, Fig. 1(a), indicating smooth, 2D growth. For the Ge_{1-x}C_x active layer, the observed evolution of RHEED patterns depended on the substrate temperature. At 215 °C, the 2×2 reconstruction remained stable and streaky throughout the growth. However, for higher growth temperatures (270 and 324 °C), the first few monolayers (MLs) initially showed 2 × 2 streaky patterns but slowly became spotty, indicating a rough surface. Figures 1(a)-1(c) show RHEED patterns observed during the growth of $Ge_{1-x}C_x$ at these temperatures.

To better understand the RHEED results, we did ex situ atomic force microscopy (AFM), shown in Figs. 1(d)-1(f). The Ge₁ -xCx film grown at 215 °C exhibited very low surface roughness of 0.63 nm RMS over a $5 \times 5 \mu m$ area. Samples grown at 270 and 324 ° C showed significantly higher RMS roughness, 8.6 and 7.5 nm, respectively, consistent with the RHEED results.

To study how surface profiles correlated with composition and crystal quality, high-resolution XRD (HRXRD) scans were measured on the symmetric (004) plane using a Rigaku SmartLab x-ray diffractometer. Figure 2 shows the (004) $2\theta/\omega$ scans of $Ge_{1-x}C_x$ as a function of growth temperature. All sample peak positions were compared with nonintentionally doped Ge layers grown at T = 433 °C as a baseline. The sharp peaks at 66.05° correspond to the GaAs substrate. The Ge_{1-x}C_x peak was observed at a higher diffraction angle, consistent with its smaller lattice constant relative to the GaAs substrate. We found that the peak position of the Ge-C (004) plane shifts by 0.23°, 0.24°, and 0.26° toward the larger angle at respective growth temperatures of 215, 270, and 324 °C, respectively, suggesting slightly increased substitutional carbon incorporation with increasing growth temperature. Fitting the XRD curves [Fig. 3(a)] using Rigaku GlobalFit showed the substitutional C percentage to be roughly 0.72%-0.75% for all three growth temperatures. Interestingly, the Ge-Ge_{1-x}C_x peak separation then decreased with further increases in growth temperature. It eventually vanished after 379 °C (not shown), consistent with segregation of C at higher growth temperatures.^{27,30} The lowest full width half maximum (FWHM) of 0.05° was observed for the sample grown at 215 °C.

Sharp Pendellösung fringes on the same sample confirmed sharp interface boundaries and a smooth surface, consistent with RHEED and AFM measurements. With increasing growth temperature, the Ge_{1-x}C_x diffraction broadened, with a maximum FWHM of 0.15° at a growth temperature of 324 °C. It is noteworthy that the

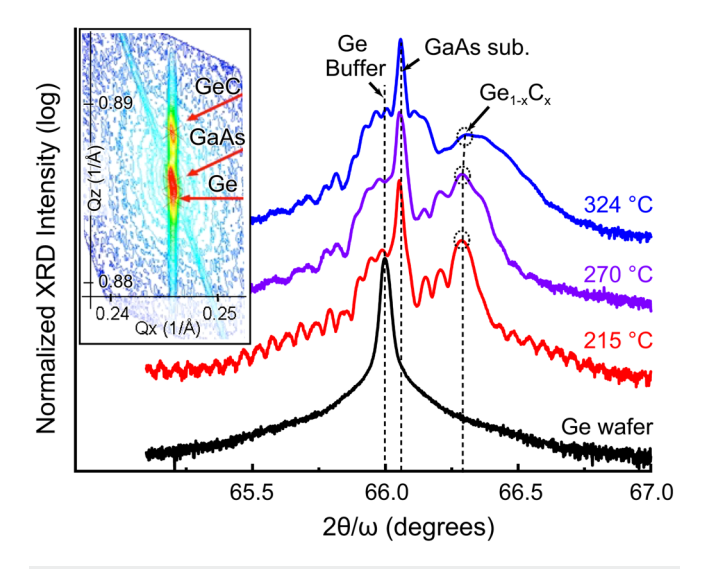


FIG. 2. HR-XRD 2θ - ω scans about GaAs (004) as a function of T_{sub} = 215-324 °C. (inset) RSM around the (115) plane for the sample at 215 °C.

Pendellösung fringes began to disappear at higher growth temperatures, consistent with the comparatively rough surface observed in RHEED and AFM. We tentatively attribute this to increased surface segregation by C at higher temperatures, leading to 3D island for-

segregation by C at higher temperatures, leading to 3D island formation, C-C defects, ^{27,30} and larger carbon clusters during growth.

To test for strain relaxation, reciprocal space mapping (RSM) was performed on all samples around the asymmetric (115) reflection. Figure 2 (inset) shows a representative RSM of $Ge_{1-x}C_x$



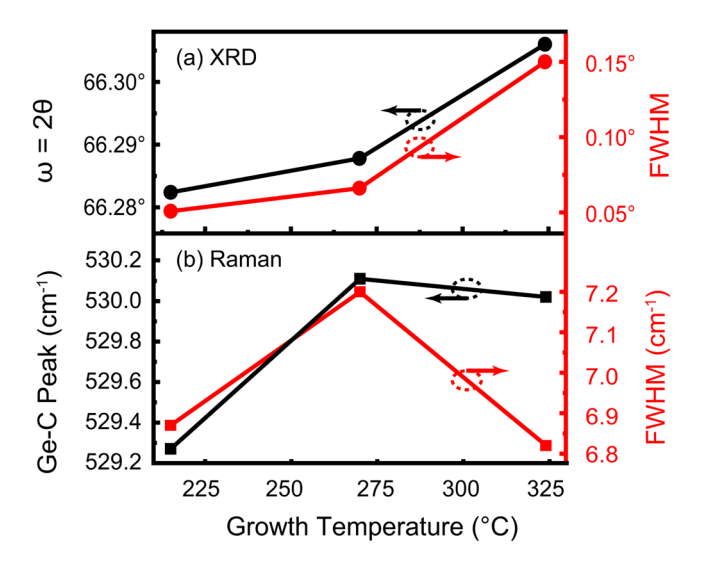


FIG. 3. (a) XRD Ge-C ω/2θ peak position and FWHM with growth temperature, fitted from Fig. 2. (b) Ge-C Raman peak position and linewidth.

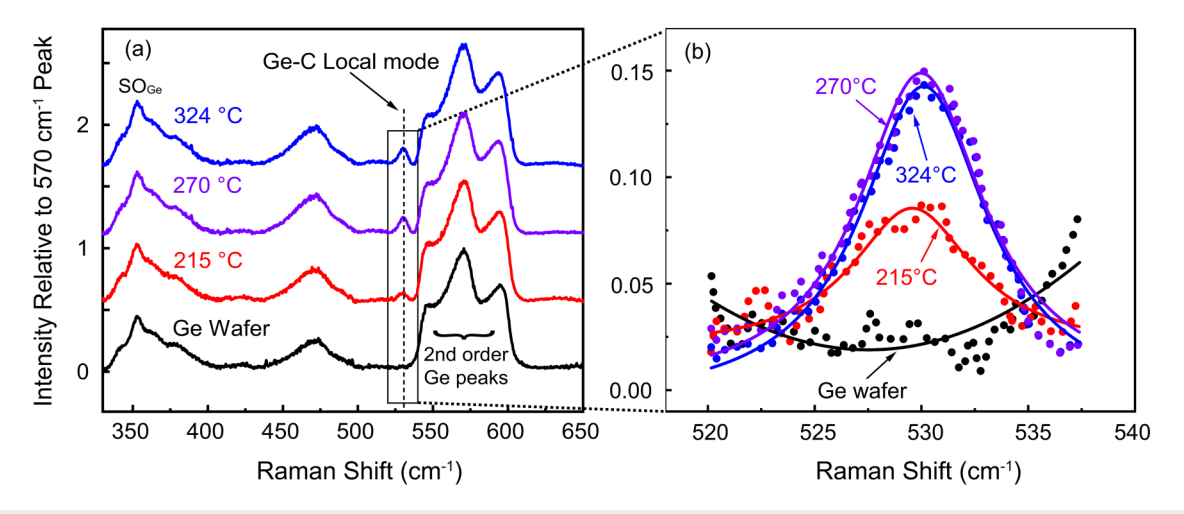


FIG. 4. (a) Raman spectra vs growth temperature (offset vertically for clarity). (b) Raman spectra and fits to the Ge-C local vibration mode near 530 cm⁻¹ after subtracting backgrounds

grown at 215 °C, where the substrate and the film peaks are vertically aligned along the same Qx (reciprocal spacing parallel to the surface), indicating the Ge buffer and Ge1-xCx alloy layers are pseudomorphic, with no detectable in-plane strain relaxation.

To further validate the XRD results and study the bonding of C in the lattice, Raman measurements were performed using a Horiba LabRam HR Evolution microscope with 532 nm excitation. At 532 nm laser wavelength, the optical penetration depth is roughly $d_{opt} \propto 1/\alpha \approx 20$ nm in Ge, 41 where α is the absorption coefficient. If we assume a similar or stronger absorption coefficient for the same pump beam in $Ge_{1-x}C_x$ at low x, then the majority of Raman signal will originate from the alloy and Ge cap. Spectra from the alloy samples exhibited a sharp mode near 530 cm⁻¹ that has been previously identified as the Ge-C local vibrational Observation of this band directly confirms the desired substitutional carbon incorporation. Based on fits to the data, the Ge-C local mode varies in position between 529.3 and 530.1 cm⁻¹, with FWHM between 6.80 and 7.20 cm⁻¹. The positions and line width are in good agreement with prior reports.

Figure 4 shows the Raman measurements near the Ge-C local vibrational mode (LVM). The measurements were unpolarized, so the first c-Ge line, Ge-C local mode, and the broad, second-order band near 575 cm⁻¹ from the Ge optical branch are all present in the spectra shown. As expected, all Raman spectral features in Ge are also present in the GeC samples because of the large fraction of Ge. We did not observe any new peaks, nor increases in existing peaks, except for a new, narrow line at 530 cm⁻¹, which is attributed to the LVM of Ge-C. 42,43 The Ge-C mode in Fig. 4 had a FWHM of $\sim 6 \text{ cm}^{-1}$ [see Fig. 3(b)], roughly consistent for all three samples grown at various temperatures. To remove the broad background caused by the second order Ge mode, a reference spectrum from pure Ge was subtracted from the Raman spectra for Fig. 4(b), followed by a fit with a single Lorentzian function for the Ge-C local vibrational mode (LVM). The reduction by half in the LVM intensity in Fig. 4(b) suggests roughly half as much carbon was incorporated substitutionally at 215 °C compared with 270 and 324 °C. It is not known whether the remaining carbon desorbed or incorporated as non-substitutional defects, but as described above, new C-C bonds were not detectable in the Raman spectra.

The Ge–Ge bands near 300 cm^{-1} in the alloy spectra may have been blue shifted from that of the reference Ge material by approximately $\Delta \omega = +0.2 \text{ cm}^{-1}$ based on fits using Lorentzian line shapes, as shown in Fig. 5. Only a small shift is expected, due to opposing contributions from the substrate-induced biaxial tensile 2 strain (red shift) and the effect of alloying on the vibrational band & structure (blue shift), and may be written as

$$\Delta \omega = \Delta \omega_{bi} + \Delta \omega_{\text{alloy}}.$$
 (1)

The XRD data indicate a tensile strain of +0.1% (±0.01%). Using the dependence on strain previously reported, 44 0.1% strain would produce a phonon redshift of $\Delta \omega_{bi} = -0.2 \, \mathrm{cm}^{-1}$. Based on Eq. (1), the alloy-induced blue shift appears to be approximately $\Delta\omega_{alloy} \approx +0.4 \, \mathrm{cm}^{-1}$. However, the spectral dispersion of the Raman system was 0.35 cm⁻¹/pixel, so even after fitting over multiple pixels, the estimated error bars are also roughly 0.2 cm⁻¹, so there is corresponding uncertainty in the actual alloy-induced blueshift.

Previous Raman reports on germanium carbide alloys showed substantial intensity from disordered C phases. 45,46 The presence of these phases was attributed to excess C accumulating at the surface rather than the desired substitutional incorporation on to $Ge_{1-x}C_x$ during growth. The signature broad bands from these materials, whether sp² or sp³ coordinated, are in the 1300 to 1600 cm⁻¹ range. Due to the sensitivity of Raman to adventitious hydrocarbons on the surface, it is difficult to completely rule out C-C bonds in the GeC film. However, no broad features were detectable from 1300 to 1600 cm⁻¹, and the sole remaining sharp peak near

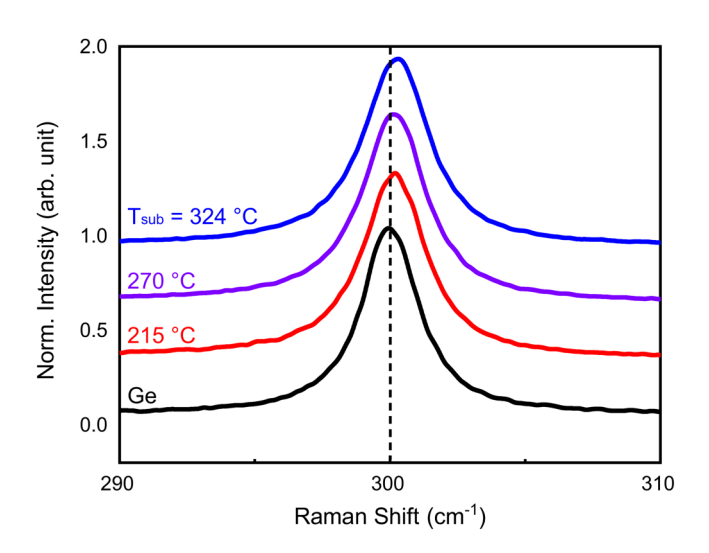


FIG. 5. First order Ge–Ge $O(\Gamma)$ Raman peak for GeC samples grown at different T_{sub}. Plots are vertically offset for clarity.

1560 cm⁻¹ (possibly a graphene like G line) was no higher in the GeC films than in a piece of Ge wafer. However as shown in Fig. 6, there were no Raman peaks visible in this range. We conclude that there is little if any graphitic carbon in these samples, nor residual C on the surface following growth.

Although XRD and Raman were consistent with highly substitutional carbon incorporation, photoluminescence was somewhat more ambiguous. Low temperature micro-PL was performed to look for the expected reduction in direct bandgaps. The sample was

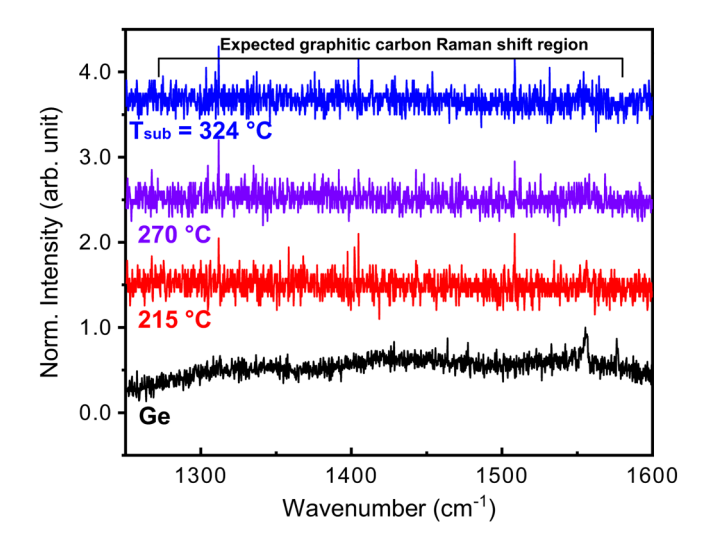


FIG. 6. Raman spectra of GeC samples grown at different T_{sub} in region of expected amorphous and graphitic sp² C-C bonds. Plots are offset vertically for clarity. A piece of Ge wafer left in air shows results of adventitious carbon.

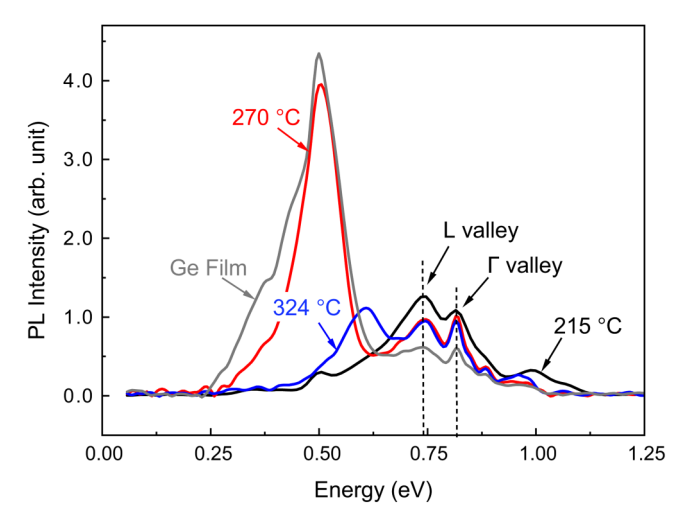


FIG. 7. LTPL spectra measured at 80 K from Ge_{1-x}C_x grown at different T_{sub}, along with Ge thin films grown at 390 °C.

mounted in a temperature-controlled cryostat with a ZnSe window. Optical pumping was provided by a 1 W, 808 nm laser modulated at 10 kHz. The pump beam passed through a 3 µm dichroic beam splitter and was focused onto the sample using an all-reflective objective. PL emitted from the sample was collected by the same objective and reflected by the dichroic beamsplitter through an AR-coated (3–5 μ m) Si window to block the laser. A liquid nitrogen \aleph cooled InSb detector was read using a lockin amplifier. For spectrally resolved IR, the PL beam was passed through a Fourier transform infrared (FTIR) setup after being reflected from the dichroic & to dramatically reduce infrared background. The average incident power at the sample was approximately 240 mW, focused into an ellipse of $200 \times 40 \,\mu\text{m}^2$.

Weak PL at 80 K was observed at 0.61 eV from the film grown at 324 °C (Fig. 7). Almost no Ge_{1-x}C_x PL was visible from the 215 °C sample, but only the direct and indirect emission from Ge. We attribute the lack of PL from the GeC layer to point defects such as vacancies induced by low temperature growth. The use of Sn and atomic H surfactants to reduce these point defects will be reported elsewhere.^{7,47} The sample grown at 270 °C shows relatively strong emission at 0.5 eV. However, we also observed similar emissions from Ge grown at 412 °C. Therefore, we cannot rule out defect-mediated emission for this peak, possibly associated with dislocation defects in Ge. If it were from point defects one might expect the highest intensity to occur either at lower temperatures where Ge vacancies are more likely, or higher temperatures where carbon segregation is more likely.⁴⁸ Preliminary x-ray photoemission spectroscopy (XPS) depth profiling suggests possible oxygen contamination in the Ge_{1-x}C_x layer for these samples, but this does not explain the maximum PL occurring at the intermediate growth temperature. Based on previous theoretical calculations by D'Arcy-Gall and others, it seems likely that annealing would generate additional carbon-carbon point defects rather than eliminate them.²⁶ However, this has not been

examined here yet in practice, but such annealing studies are currently under way. Further growths are now under way after eliminating several possible contaminants from the CBr_4 gas lines, and to identify possible point defects in the $Ge_{1-x}C_x$ layers.

At these low growth temperatures, we do not expect significant diffusion of Ga or As into the subsequent Ge or GeC layers, which has subsequently been verified by SIMS of similar samples. Also, even if there were some amount of dopant diffusion, this would not change the results presented here. Indeed, it might accelerate device development by providing mutual n-type doping across the Ge–GaAs interface without needing to add toxic or contaminating n-dopants such as arsenic or phosphine in the growth chamber.

IV. SUMMARY

In summary, we showed successful incorporation of C in Ge as tin-free $Ge_{1-x}C_x$ using CBr_4 as a C precursor. HRXRD showed a tensile strained layer corresponding to a minimum of 0.76% of substitutional C in $Ge_{1-x}C_x$ at $T_{sub}=324\,^{\circ}C$, consistent with an increase in the G–C local mode in the Raman spectrum. Raman also showed no amorphous or graphitic C. RHEED, AFM, and XRD measurements indicated smooth surfaces and better crystal quality at $T_{sub}=215\,^{\circ}C$, but this temperature had the weakest PL. However, even without Sn or H surfactants, PL was demonstrated at 0.5 and 0.61 eV from the samples grown at 270 and 324 °C, respectively, consistent with the expected wavelength from this concentration of C. This suggests direct bandgap, group IV light emitters for silicon photonics might be possible using inexpensive, commercially available carbon precursors.

ACKNOWLEDGMENTS

This work was supported in part by the National Science Foundation (NSF) under Grant Nos. DMR-1508646, CBET-1438608, and DMR-2122041, and by the Analysis Research Service Center (ARSC) and LEAP cluster at Texas State University.

AUTHOR DECLARATIONS

Conflict of Interest

The authors have no conflicts to disclose.

Author Contributions

Md. Shamim Reza: Formal analysis (equal); Investigation (equal); Resources (equal); Writing – original draft (lead). Tuhin Dey: Conceptualization (supporting); Investigation (supporting); Methodology (supporting); Resources (equal). Augustus W. Arbogast: Conceptualization (supporting); Investigation (supporting); Resources (equal). Aaron J. Muhowski: Investigation (supporting). Mark W. Holtz: Conceptualization (supporting); Formal analysis (supporting); Methodology (supporting); Writing – review & editing (equal). Chad A. Stephenson: Conceptualization (supporting). Seth R. Bank: Funding acquisition (supporting); Supervision (supporting). Daniel Wasserman: Funding acquisition (supporting); Supervision (supporting); Supervision (supporting), Supervision (supporting). Mark A. Wistey: Conceptualization

(lead); Funding acquisition (lead); Methodology (equal); Resources (equal); Supervision (lead); Writing – review & editing (equal).

DATA AVAILABILITY

The data that support the findings of this study are available from the corresponding author upon reasonable request.

REFERENCES

- ¹X. Sun, J. Liu, L. C. Kimerling, and J. Michel, "Toward a germanium laser for integrated silicon photonics," IEEE J. Sel. Top. Quantum Electron. **16**(1), 124–131 (2010).
- ²J. Liu, X. Sun, R. E. Camacho-Aguilera, L. C. Kimerling *et al.*, "Ge-on-Si laser operating at room temperature," Opt. Lett. 35(5), 679–681 (2010).
- ³S. Bao, D. Kim, C. Onwukaeme, S. Gupta, K. Saraswat, K. H. Lee, Y. Kim, D. Min, Y. Jung, H. Qiu, H. Wang, E. A. Fitzgerald, C. S. Tan, and D. Nam, "Low-threshold optically pumped lasing in highly strained germanium nanowires," Nat. Commun. 8(1), 1845 (2017).
- ⁴J. Petykiewicz, D. Nam, D. S. Sukhdeo, S. Gupta, S. Buckley, A. Y. Piggott, J. Vučković, and K. C. Saraswat, "Direct bandgap light emission from strained germanium nanowires coupled with high-Q nanophotonic cavities," Nano Lett. 16(4), 2168–2173 (2016).
- ⁵N. Von Den Driesch, D. Stange, S. Wirths, G. Mussler, B. Holländer, Z. Ikonic, J. M. Hartmann, T. Stoica, S. Mantl, D. Grützmacher, and D. Buca, "Direct bandgap group IV epitaxy on Si for laser applications," Chem. Mater. 27(13), 4693–4702 (2015).
- ⁶R. A. Soref and L. Friedman, "Direct-gap Ge/GeSn/Si and GeSn/Ge/Si heterostructures," Superlattices Microstruct. 14(2–3), 189–193 (1993).
- ⁷T. Dey, M. S. Reza, A. Arbogast, M. W. Holtz, R. Droopad, S. R. Bank, and M. A. Wistey, "Molecular beam epitaxy of highly crystalline GeSnC using CBr4 at low temperatures," Appl. Phys. Lett. 121(12), 122104 (2022).
- 8E. A. Fitzgerald, P. E. Freeland, M. T. Asom, W. P. Lowe, R. A. Macharrie, B. E. Weir, A. R. Kortan, F. A. Thiel, Y.-H. Xie, A. M. Sergent, S. L. Cooper, G. A. Thomas, and L. C. Kimerling, "Epitaxially stabilized Ge_xSn_{1-x} diamond cubic alloys," J. Electron. Mater. 20(6), 489–501 (1991).
- ⁹C. A. Stephenson, W. A. O'Brien, M. W. Penninger, W. F. Schneider, & M. Gillett-Kunnath, J. Zajicek, K. M. Yu, R. Kudrawiec, R. A. Stillwell, and M. A. Wistey, "Band structure of germanium carbides for direct bandgap silicon photonics," J. Appl. Phys. 120(5), 053102 (2016).
- ¹⁰I. A. Gulyas, C. A. Stephenson, Q. Meng, S. R. Bank, and M. A. Wistey, "The carbon state in dilute germanium carbides," J. Appl. Phys. **129**(5), 055701 (2021).
- ¹¹X. Sun, J. Liu, L. C. Kimerling, and J. Michel, "Room-temperature direct bandgap electroluminesence from Ge-on-Si light-emitting diodes," Opt. Lett. **34**(8), 1198 (2009).
- ¹²J. Liu, R. Camacho-Aguilera, J. T. Bessette, X. Sun, X. Wang, Y. Cai, L. C. Kimerling, and J. Michel, "Ge-on-Si optoelectronics," Thin Solid Films 520(8), 3354–3360 (2012).
- ¹³J. Jiang, M. Xue, C.-Y. Lu, C. S. Fenrich, M. Morea, K. Zang, J. Gao, M. Cheng, Y. Zhang, T. I. Kamins, J. S. Harris, and J. Sun, "Strain-induced enhancement of electroluminescence from highly strained germanium light-emitting diodes," ACS Photonics 6(4), 915–923 (2019).
- ¹⁴M. el Kurdi, G. Fishman, Ś Sauvage, and P. Boucaud, "Band structure and optical gain of tensile-strained germanium based on a 30 band kp formalism," J. Appl. Phys. **107**(1), 013710 (2010).
- 15S. Wirths, A. T. Tiedemann, Z. Ikonic, P. Harrison, B. Holländer, T. Stoica, G. Mussler, M. Myronov, J. M. Hartmann, D. Grützmacher, D. Buca, and S. Mantl, "Band engineering and growth of tensile strained Ge/(Si)GeSn heterostructures for tunnel field effect transistors," Appl. Phys. Lett. 102(19), 192103 (2013).
- ¹⁶M. Qi, W. O'Brien, C. A. Stephenson, V. Patel, N. Cao, B. Thibeault, M. Schowalter, A. Rosenauer, V. Protasenko, H. Xing, and M. Wistey, "Extended

- defect propagation in highly tensile-strained Ge waveguides," Crystals 7(6), 157 (2017).
- ¹⁷J. Zheng, Z. Liu, C. Xue, C. Li, Y. Zuo, B. Cheng, and Q. Wang, "Recent progress in GeSn growth and GeSn-based photonic devices," J. Semicond. 39(6), 061006 (2018).
- ¹⁸S. A. Ghetmiri, W. Du, J. Margetis, A. Mosleh, L. Cousar, B. R. Conley, L. Domulevicz, A. Nazzal, G. Sun, R. A. Soref, J. Tolle, B. Li, H. A. Naseem, and S.-Q. Yu, "Direct-bandgap GeSn grown on silicon with 2230 nm photoluminescence," Appl. Phys. Lett. 105(15), 151109 (2014).
- 19Y. Zhou, Y. Miao, S. Ojo, H. Tran, G. Abernathy, J. M. Grant, S. Amoah, G. Salamo, W. Du, J. Liu, J. Margetis, J. Tolle, Y. Zhang, G. Sun, R. A. Soref, B. Li, and S.-Q. Yu, "Electrically injected GeSn lasers on Si operating up to 100 K," Optica 7(8), 924 (2020).
- 20 Y. Zhou, W. Dou, W. Du, S. Ojo, H. Tran, S. A. Ghetmiri, J. Liu, G. Sun, R. Soref, J. Margetis, J. Tolle, B. Li, Z. Chen, M. Mortazavi, and S.-Q. Yu, "Optically pumped GeSn lasers operating at 270 K with broad waveguide structures on Si," ACS Photonics 6(6), 1434–1441 (2019).
- ²¹S. Al-Kabi, S. A. Ghetmiri, J. Margetis, T. Pham, Y. Zhou, W. Dou, B. Collier, R. Quinde, W. Du, A. Mosleh, J. Liu, G. Sun, R. A. Soref, J. Tolle, B. Li, M. Mortazavi, H. A. Naseem, and S.-Q. Yu, "An optically pumped 2.5 μm GeSn laser on Si operating at 110 K," Appl. Phys. Lett. 109(17), 171105 (2016).
- ²²C. A. Stephenson, W. A. O'brien, M. Qi, M. Penninger, W. F. Schneider, and M. A. Wistey, "Band anticrossing in dilute germanium carbides using hybrid density functionals," J. Electron. Mater. 45(4), 2121–2126 (2016).
- ²³R. Duschl, O. G. Schmidt, W. Winter, K. Eberl, M. W. Dashiell, J. Kolodzey, N. Y. Jin-Phillipp, and F. Phillipp, "Growth and thermal stability of pseudomorphic Ge_{1-y}Cy/Ge superlattices on Ge(001)," Appl. Phys. Lett. 74(8), 1150–1152 (1999).
- ²⁴H. J. Osten, E. Bugiel, and P. Zaumseil, "Antimony-mediated growth of epitaxial Ge_{1-y}Cy layers on Si(001)," J. Cryst. Growth **142**(3–4), 322–326 (1994).
- ²⁵M. Krishnamurthy, J. S. Drucker, and A. Challa, "Epitaxial growth and characterization of Ge1-xCx alloys on Si(100)," J. Appl. Phys. **78**(12), 7070–7073 (1995).
- ²⁶S. Y. Park, J. D'Arcy-Gall, D. Gall, Y.-W. Kim, P. Desjardins, and J. E. Greene, "C lattice site distributions in metastable $Ge_{1-y}C_y$ alloys grown on Ge(001) by molecular-beam epitaxy," J. Appl. Phys. **91**(6), 3644–3652 (2002).
- ²⁷D. Gall, J. D'Arcy-Gall, and J. E. Greene, "C incorporation in epitaxial layers grown on Ge(001): An *ab initio* study," Phys. Rev. B **62**(12), R7723–R7726 (2000).
 ²⁸J. Kolodzey, P. A. O'Neil, S. Zhang, B. A. Orner, K. Roe, K. M. Unruh,
- C. P. Swann, M. M. Waite, and S. I. Shah, "Growth of germanium-carbon alloys on silicon substrates by molecular beam epitaxy," Appl. Phys. Lett. **67**(13), 1865–1867 (1995).
- ²⁹H. J. Osten and J. Klatt, "In situ monitoring of strain relaxation during antimony-mediated growth of Ge and $Ge_{1-y}C_y$ layers on Si(001) using reflection high energy electron diffraction," Appl. Phys. Lett. **65**(5), 630–632 (1994).
- 30 J. D'Arcy-Gall, D. Gall, I. Petrov, P. Desjardins, and J. E. Greene, "Quantitative C lattice site distributions in epitaxial $Ge_{1-y}C_y/Ge(001)$ layers," J. Appl. Phys. 90(8), 3910–3918 (2001).
- ³¹M. W. Dashiell, J. Kolodzey, P. Boucaud, V. Yam, and J.-M. Lourtioz, "Heterostructures of pseudomorphic $Ge_{1-y}C_y$ and $Ge_{1-x-y}Si_xC_y$ alloys grown on Ge (001) substrates," J. Vac. Sci. Technol., B **18**(3), 1728 (2000).
- ³²R. Schaeffer and R. K. Pearson, "Reaction of carbon vapor produced by laser evaporation of graphite," J. Am. Chem. Soc. 91(8), 2153–2154 (1969).

- ³³J. Berkowitz and W. A. Chupka, "Mass spectrometric study of vapor ejected from graphite and other solids by focused laser beams," J. Chem. Phys. **40**(9), 2735–2736 (1964).
- ³⁴E. A. Rohlfing, D. M. Cox, and A. Kaldor, "Production and characterization of supersonic carbon cluster beams," J. Chem. Phys. **81**(7), 3322–3330 (1984).
- ³⁵R. E. Honig, "Mass spectrometric study of the molecular sublimation of graphite," J. Chem. Phys. **22**(1), 126–131 (1954).
- ³⁶J. M. Hwang, D. K. Schroder, and W. J. Biter, "Deep levels introduced into silicon during hydrogen plasma annealing," J. Appl. Phys. 57(12), 5275–5278 (1985).
- ³⁷M. A. Wistey, S. R. Bank, H. B. Yuen, J. S. Harris, Jr., M. M. Oye, and A. L. Holmes, Jr., "Using beam flux monitor as Langmuir probe for plasma-assisted molecular beam epitaxy," J. Vac. Sci. Technol., A 23(3), 460–464 (2005).
- ⁵⁸M. A. Wistey, S. R. Bank, H. B. Yuen, H. Bae, and J. S. Harris, "Nitrogen plasma optimization for high-quality dilute nitrides," J. Cryst. Growth **278**(1), 229–233 (2005).
- ³⁹J. Kouvetakis, A. Haaland, D. J. Shorokhov, H. V. Volden, G. V. Girichev, V. I. Sokolov, and P. Matsunaga, "Novel methods for CVD of Ge₄C and (Ge₄C)_xSi_y diamond-like semiconductor heterostructures: Synthetic pathways and structures of trigermyl-(GeH₃)₃CH and tetragermyl-(GeH₃)₄C methanes," J. Am. Chem. Soc. 120(27), 6738–6744 (1998).
- ⁴⁰C. A. Stephenson, M. Gillett-Kunnath, W. A. O'Brien, R. Kudrawiec, and M. A. Wistey, "Gas source techniques for molecular beam epitaxy of highly mismatched Ge alloys," Crystals **6**(12), 159 (2016).
- ⁴¹D. E. Aspnes and A. A. Studna, "Dielectric functions and optical parameters of Si, Ge, GaP, GaAs, GaSb, InP, InAs, and InSb from 1.5 to 6.0 eV," Phys. Rev. B **27**(2), 985–1009 (1983).
- ⁴²W. H. Weber, B.-K. Yang, and M. Krishnamurthy, "The Ge-C local mode in epitaxial GeC and Ge-rich GeSiC alloys," Appl. Phys. Lett. 73(5), 626–628 (1998).
- ⁴³Y. Kanzawa, K. Katayama, K. Nozawa, T. Saitoh, and M. Kubo, "Preparation of Ge_{1-γ}C_γ alloys by C implantation into Ge crystal and their Raman spectra," [2] Jpn. J. Appl. Phys. **40**(10), 5880–5884 (2001).
- Jpn. J. Appl. Phys. **40**(10), 5880–5884 (2001).

 44C.-Y. Peng, C.-F. Huang, Y.-C. Fu, Y.-H. Yang, C.-Y. Lai, S.-T. Chang, and C. W. Liu, "Comprehensive study of the Raman shifts of strained silicon and germanium," J. Appl. Phys. **105**(8), 83537 (2009).
- ⁴⁵B.-K. Yang, M. Krishnamurthy, and W. H. Weber, "Incorporation and stability of carbon during low-temperature epitaxial growth of $Ge_{1-x}C_x$ (x<0.1) alloys on Si(100): Microstructural and Raman studies," J. Appl. Phys. **82**(7), 3287–3296 (1997)
- ⁴⁶M. Krishnamurthy, B.-K. Yang, and W. H. Weber, "Microstructural development and optical properties of epitaxial $Ge_{1-x}C_x$ alloys on Si(100)," Appl. Phys. Lett. **69**(17), 2572–2574 (1996).
- ⁴⁷T. Dey, A. W. Arbogast, Q. Meng, M. S. Reza, A. J. Muhowski, J. Cooper, T. Borrely, E. Ozdemir, F. U. Naab, R. S. Goldman, S. R. Bank, M. W. Holtz, and M. A. Wistey, "Influence of H Sn incorporation into GeSnC alloy," J. Appl. Phys. (in press, 2023).
- ⁴⁸M. Kittler, T. Arguirov, M. Oehme, Y. Yamamoto, B. Tillack, and N. V. Abrosimov, "Photoluminescence study of Ge containing crystal defects," Phys. Status Solidi (A) 208(4), 754–759 (2011).